Recent Results of LID Experiment on LHD

T. Morisaki, S. Masuzaki, M. Kobayashi, R. Sakamoto, K. Tanaka, K. Narihara, H. Funaba, Y. Feng[1], F. Sardei[1], N. Ohyabu, A. Komori, O. Motojima and LHD Experimental Group
Nationao Institute for Fusion Science, Toki, Gifu 509-5292, Japan
[1]*Max-Planck-Institute fuer Plasmaphysik, EURAROM Association, D-17941, Greifswald, Germany*

1. Introduction

In the Large Helical Device (LHD) project [1], divertor research is one of the most important goals in the mission to achieve high quality helical plasmas relevant to a fusion reactor. The divertor is expected to play a key role in improving the plasma performance through edge control.

In LHD, two completely different divertor magnetic geometries are employed, i.e., the helical divertor (HD) and the local island divertor (LID). The HD is similar to the tokamak double null divertor except for the long connection length of the field lines in the thick ergodic region surrounding the closed surfaces [2]. The LID is an alternative, innovative concept [3] utilized for edge plasma control, prior to the full-scale HD operation.

2. LID principle and experimental setup

The LID is a kind of the island divertor [4] which utilizes a superimposed *m/n*=1/1 island located in the edge region, where *m* and *n* are poloidal and toroidal mode numbers, respectively. By inserting the LID head into the island from the outboard side of the torus, field lines of the island are cut by the LID head, thus removing all closed flux surfaces around the edge region.

Particles diffusing out from the core region cross the island separatrix and flow along the periphery of the island. After several toroidal turns, they reach the outer separatrix of the island where the LID head is placed, and strike its backside on which they are neutralized, as shown in Fig. 1. Since the LID head is inserted deeply in the island, the leading edge of the head is safe from high heat flux. Particles recycled there are pumped out efficiently by the strong pumping system with a baffle integrated into the closed divertor configuration. Note that LID is not a pumping limiter but a genuine divertor, because the LID head never scrapes off plasma from the confinement region. In the LID configuration, the boundary of the confinement region is defined with the inner island separatrix.

The LID system consists of two parts, i.e., the perturbation coils and the LID head system. For generating an *m/n*=1/1 island, ten pairs of small loop coils are installed at the top and bottom of the torus. Three power supplies drive these coils, and can generate a 0.23 m wide island at the position where the LID head is located. The LID head system consists mainly of a divertor head surrounded with a baffle, vacuum pumps and a translation mechanism. The LID head whose size is about 1m × 0.6m × 0.4m has a highly complicated three dimensional (3D) shape to fit into the island structure. The surface of the LID head is covered with carbon and partially with molybdenum tiles to withstand the high heat loads. The tiles are mechanically joined to a stainless steel heat sink on which water cooling channels are grooved. Thin carbon sheets are sandwiched between the tiles and the heat sink to increase the contact area. The divertor head is surrounded by a baffle to realize a closed

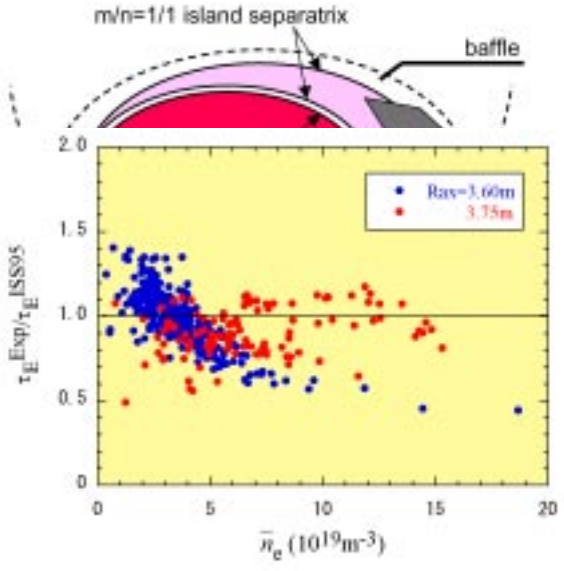

Fig. 2 Dependence of improvement factor from the ISS95 scaling on line averaged density $\bar{n}$.

divertor system. Some diagnostics are built into the LID head system. For flux measurements 39 Langmuir probes and 22 thermocouples are embedded in the carbon tiles. Image guide fibers for two dimensional profile measurements and a bundle fiber for visible spectroscopy are also installed inside the baffle, viewing the divertor head from its backside. In order to estimate the pumping efficiency, an ASDEX style gauge is installed inside the baffle. By using the eight cryogenic pumps, an effective hydrogen pumping speed of 111m^3/sec at the gate valve between LHD and the LID chamber is achieved.

3. Experimental results

3.1 LID basic functions

In the early stage of LID experiments, basic functions of LID as a "divertor" have been confirmed, i.e. particle flow along the island separatrix, profile control in the edge region, impurity control, etc [5,6]. The pumping efficiency of about 40% was also estimated experimentally.

3.2 Confinement properties

In the HD configuration, LHD has its best confinement performance in the R_{ax}= 3.60m configuration, where R_{ax} is the magnetic axis position [7]. Following this experimental result, LID was designed for the R_{ax}= 3.60m configuration and the experiment was performed at R_{ax}= 3.60m, at the beginning. As shown in Fig. 2, the confinement performance of LID at R_{ax}= 3.60m shows similar trend to that of HD [8], i.e. the confinement performance degrades as $\bar{n}$ increases. In the $\bar{n}$ range up to ~ 4 x $10^{19}$$m^{-3}$ for most of LID discharges, the improvement factor from the ISS95 [9] scaling is less than unity, although the edge plasma is well controlled by LID with strong pumping effect, thus the steep edge T_e gradient is formed at the edge region, as mentioned in section 3.1 [5].

Investigating new operational regime to achieve better confinement performance, a favorable configuration for LID has been found at R_{ax}= 3.75m. In this configuration, the confinement performance does not degrade so much with the increase in $\bar{n}$, and the improvement factor from the ISS95 scaling is kept around unity all though the density range, as shown in Fig. 2. Even in the high density regime above $\bar{n}$ ~ 1 x

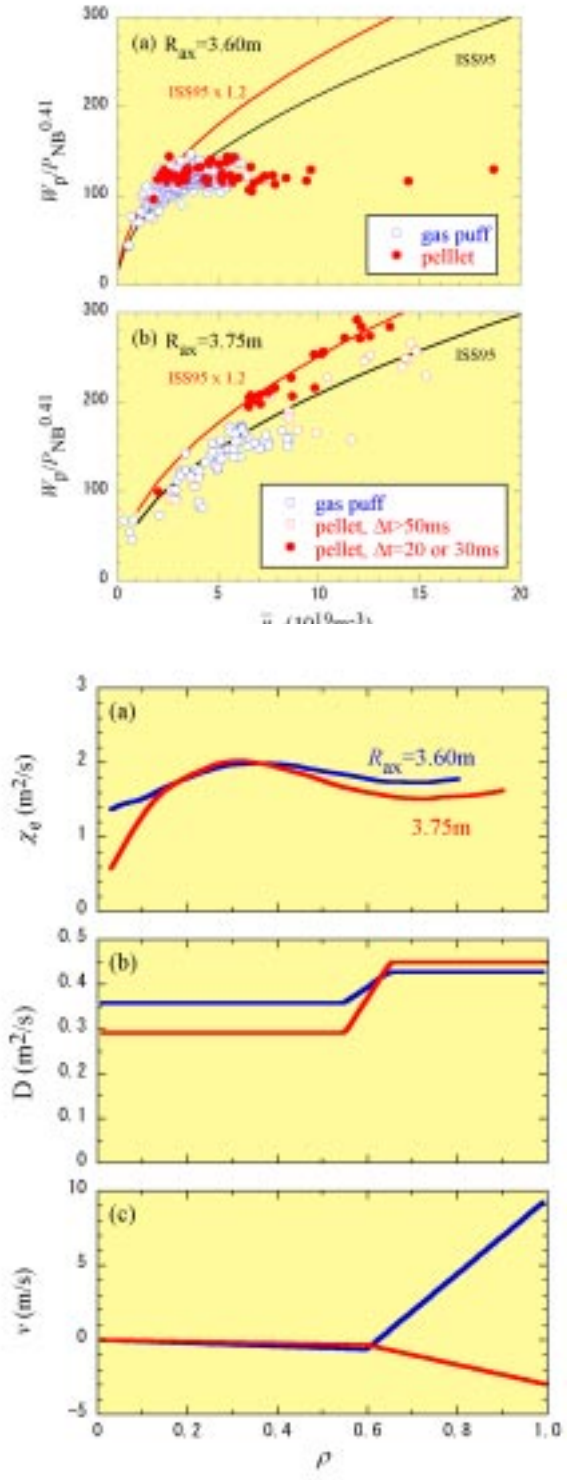

Fig. 5 Radial profiles of (a) electron heat conductivity, (b) diffusion coefficient and (c) convection velocity for R_{ax} = 3.60m (blue) and

$10^{20}m^{-3}$, some discharges with improvement factor of ~ 1.2 are obtained. In such a high density regime, the hydrogen pellet injection is employed for the deeper fueling instead of ordinary gas puffing. With the pellet injection, operational density range can be extended further than gas puffing in both configurations.

Different fueling methods show different confinement properties, especially at R_{ax}= 3.75m. Figure 3 presents density dependence of plasma stored energy W_p normalized by the $P_{NB}^{0.41}$ for the comparison with ISS95 scaling, where W_p and P_{NB} is the plasma stored energy measured with diamagnetic loops and absorbed NB (neutral beam injection) power, respectively. Different symbols in the figure represent different fueling methods. It can clearly be seen in Fig.3 (a) that $W_p/P_{NB}^{0.41}$ at R_{ax}= 3.60m is completely saturated in $\bar{n}_e$ > 3 x $10^{19}m^{-3}$ even with the pellet injection, although achieved $\bar{n}_e$ becomes high. On the other hand, at R_{ax}= 3.75m, saturation of $W_p/P_{NB}^{0.41}$ cannot be seen in discharges with the pellet injection. The $W_p/P_{NB}^{0.41}$ continuously increases with $\bar{n}_e$, following the ISS95 scaling by the deep fueling with the repetitive pellet injection with the interval, Δt, more than 50ms. Shortening the repetitive period less than 30ms, the confinement property changes its stage, as shown in Fig. 3 (b). The $W_p/P_{NB}^{0.4}$ keeps increasing, following the 20% improved curve from the ISS95 scaling. No difference is seen between long (Δt > 50ms) and short (Δt < 30ms) repetitive periods at R_{ax}= 3.60m, i.e. the confinement always degrades from the ISS95 scaling in the high density regime with the pellet injection.

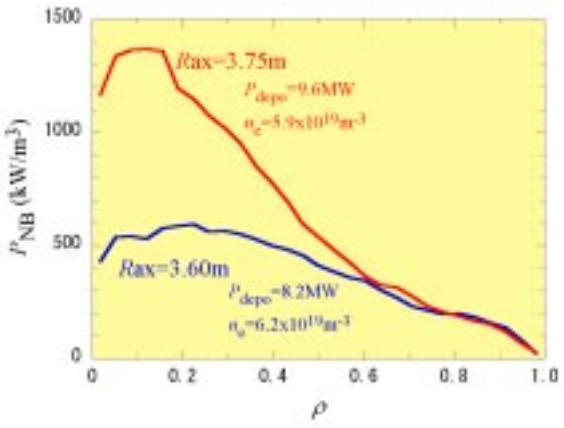

Fig. 6 Power deposition profiles in NB heated plasma.

The improved confinement regime with the frequent (Δt < 30ms) repetitive pellet injection at R_{ax}= 3.75m is achieved in the "reheat" mode after turning off the gas puff and pellet injection. At that time very interesting n_e and T_e profiles appears, as shown in Fig. 4. The highly peaked n_e profile, accompanied by the peaked T_e profile, is achieved, which has not been seen in pellet discharges in the HD configuration. It can be seen that the position where the n_e and T_e gradients become steep is corresponding to the rational surface at q=2. The large Shafranov shift seen in Fig. 4 also convinces us of the high pressure at the center.

In order to investigate the reason for the better performance at R_{ax}= 3.75m, transport analyses have been performed to get the information about the electron heat conductivity, χ_e, diffusion coefficient D and convection velocity, v. Deriving χ_e, a 3D Monte Carlo simulation code [10] was employed. For D and v, density modulation experiments were performed. It can be seen that there exists no clear difference in χ_e and D for both configurations. On the other hand, the direction of v at R_{ax}= 3.75m is inward, opposite to R_{ax}= 3.60m in the edge region, which may be a reason for the better confinement and density peaking at R_{ax}= 3.75m. Furthermore peaked NB power deposition profile at R_{ax}= 3.75m also supports its superiority of confinement performance, as shown in Fig. 6.

3.3 Numerical analyses for parallel temperature gradient

In the LID configuration, it is found from the experimental result that there exists a relatively large temperature drop along the divertor SOL (Scrape Off Layer) from the stagnation point to

the target plate. Figure 7 shows the dependence of the electron temperature at the inner separatrix, T_{eu}, and at the LID head, T_{ed}, on line averaged electron density, $\bar{}$. The $\bar{}$ dependence of their ratio, T_{eu}/T_{ed}, is also depicted in the figure with another y-axis. The T_{eu} is measured with the Thomson scattering system, and T_{ed} by the embedded Langmuir probes in the LID head. It can be seen that, as $\bar{}$ increases from ~2 x 10^{19}m^{-3} to ~5 x 10^{19}m^{-3}, both T_{eu} and T_{ed} gradually decrease, being accompanied by the increase of T_{eu}/T_{ed} up to ~15. The ratio T_{eu}/T_{ed} ~15 in LID is really high compared to that observed in tokamak divertor SOLs. In the tokamak divertor SOL with the same collisionality as LID, the ratio T_{eu}/T_{ed} should be ~2, which is estimated with the simple two-point model using a pure parallel conduction energy transport. The discrepancy of T_{eu}/T_{ed} between the experiment and the simple two point model indicates that there exist other transport processes in addition to the simple parallel transport.

The result of the numerical simulation by using a fully three dimensional edge transport code called EMC3-EIRENE [11] is compared to the experimental result. Figure 8 shows the parallel electron and ion temperature profiles along the flux tube in the LID SOL, derived from the EMC3-EIRENE code. The abscissa is the length of the flux tube, L_c, from the LID head. This computation is corresponding to the experimental result of $\bar{}$ ~ 4.3 x 10^{19}m^{-3} in Fig. 7. The heating power, P_{NB} ~ 8MW from the experiment, is used for the calculation. It is found that T_e decreases from 160eV at the upstream down to 9eV at the target (LID head), resulting in T_{eu}/T_{ed} ~18, which agrees well to the experiment.

In order to know other transport processes which should not be neglected in the LID SOL, the extended two-point model with some corrections is employed as follows. Taking into account these effects, the temperature ratio scales as

$$T_{eu}/T_{ed} \quad f^{6/7}_{cond} f^{2}_{mom}/(1-f_{power})^2, \qquad (1)$$

where f_{cond} is the fraction of the energy carried by parallel conduction, which is reduced by the increase of parallel convection. The f_{mom} is a momentum loss factor defined as $2n_dT_d=f_{mom}\, n_uT_u$, which is caused by the frictional collisions with neutrals, viscous forces and volume recombination. And f_{power} is a power loss factor defined as

$$f_{power}q_{\|} = q_{rad} + q_{cx} + q_{perp}, \qquad (2)$$

where q_{rad}, q_{cx} and q_{perp} are volumetric power losses due to radiation, charge exchange and perpendicular transport. Note that all factors, f, range from zero to one. It has been found from the EMC3-EIREME result that the momentum loss is small in LID, i.e. f_{mom} ~ 1, consequently T_e cooling is effectively enhanced by the increased f_{power}, because the effect of f_{cond} is much less than that of f_{power} due to its small exponent of 6/7, as seen from Eq (1). From the experimental result

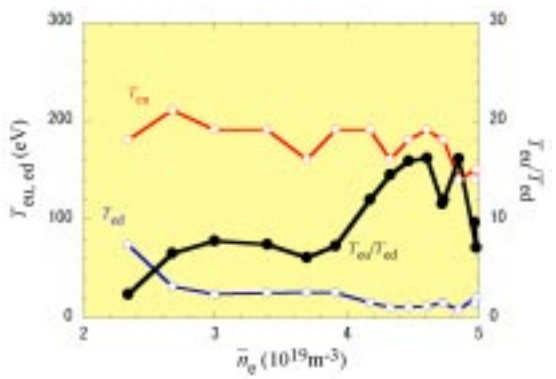

Fig. 7 Density dependence of electron temperature at the inner separatrix of the island (T_{eu}), LID head (T_{ed}) and their ratio. T_{eu} and T_{ed} are measured with Thomson scattering system and Langmuir probe, respectively.

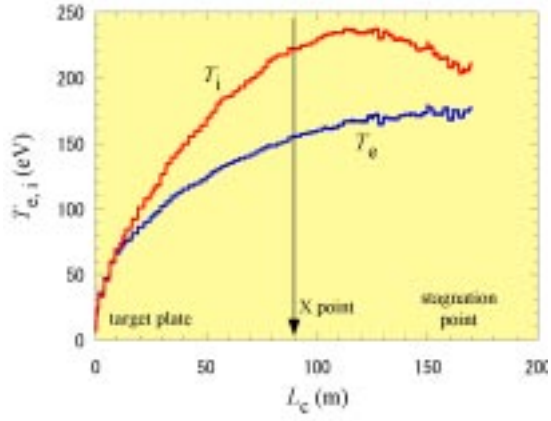

Fig. 8 Electron and ion temperature profiles along the flux tube from the stagnation point to the target plate through the X point in LID SOL obtained by EMC3-EIRENE, under the condition of $\bar{}$ ~ 4.3 x 10^{19}m^{-3} and P_{NB} ~ 8MW.

with a bolometer and the computation result with the EMC3-EIRENE code, q_{rad} and q_{cx} are found to be small. Thus it can be concluded that the dominant term that increases f_{power} is, therefore, q_{perp} (=), the energy loss via perpendicular transport. The effect of this term is estimated as follows.

When the parallel and perpendicular (conduction) terms balance in the energy equation, ~ , one can get $\kappa_{\|} T_e^{3.5}/L_c^2$ ~ , assuming the parallel and perpendicular characteristic lengths to be L_c and w, respectively. In the equation, $\kappa_{\|}$, , L_c and w are parallel and perpendicular heat conductivities, length of the flux tube in LID SOL and island width, respectively. Thus the temperature to realize this condition is given as,

—— , (3)

where Θ is a field line pitch, in the case of LID $\Theta = 0.5w/L_c$. With = $2m^2/s$ and n = 5 x $10^{19}m^{-3}$, T_{SOL} is ~ 50eV for LID, while T_{SOL} is ~ 1eV for tokamaks. One sees how significantly the perpendicular transport contributes to the energy transport in LID. It is also noted that in the LID configuration the distance between the stagnation point and the target is rather long, ~ 180m. The significant cooling along the SOL is thus considered due to the enhanced perpendicular loss along the long field lines from the stagnation point adjacent to the core plasma to the LID head.

4. Summary

The confinement performance in the LID configuration with 1.2 times improvement from the ISS95 was found at R_{ax}= 3.75m. In the regime, a highly peaked n_e profile, accompanied with a modest peaked T_e profile, is established in the reheat phase after repetitive pellet injection. Inward convective velocity and/or a peaked P_{NB} profile are experimentally found to be candidates for the improved confinement.

Numerical analyses for parallel temperature gradient revealed the characteristic feature of the LID SOL which enhances the perpendicular transport due to the long field lines in SOL.

Acknowledgements

This work is funded by MEXT of the Japanese government under Grant No. NIFS05ULPP506.

References

[1] O. Motojima, et al., Phys. Plasmas **6** (1999) 7843.
[2] N. Ohyabu, et al., Nucl. Fusion **34** (1994) 387.
[3] N. Ohyabu, et al., J. Nucl. Mater. **145-147** (1987) 844.
[4] K. McCormick, et al., J. Nucl. Mater. **313-316** (2003) 1131.
[5] T. Morisaki, et al. J. Nucl. Mater. 2005, **337-339** 154.
[6] A. Komori, et al., Nucl. Fusion **45** (2005) 837.
[7] H. Yamada *et al*, Plasma Phys. Control. Fusion **44** (2001) A55.
[8] H. Yamada *et al*, Nucl. Fusion **43** (2003) 749.
[9] U. Stroth, et al., Nucl. Fusion **36** (1996) 1063.
[10] S. Murakami, et al., Trans. Fusion Technol. **27** (1995) 256.
[11] Y. Feng et al., 2002 Plasma Phys. Control. Fusion **44** (2002) 611.